ORIGINAL ARTICLE

Thermal behavior of crimped spiral fin tube bank under dehumidifying process: A case study of inline arrangement

Atipoang Nuntaphan[1] and Tanongkiat Kiatsiriroat[2]

Abstract

Nuntaphan, A. and Kiatsiriroat, T.
Thermal behavior of crimped spiral fin tube bank under dehumidifying process: A case study of inline arrangement
Songklanakarin J. Sci. Technol., 2004, 26(4) : 509-519

Cross flow heat exchangers having crimped spiral fin and inline arrangement configurations under dehumidification are studied. The effect of tube diameter, fin spacing, fin height, transverse tube pitch are examined. From the experiment, it is found that the heat transfer and the frictional characteristics of the heat exchanger under dehumidification is close to that of the non-dehumidifying process. However, the air stream pressure drop and the heat transfer coefficient of the wet surface heat exchanger are higher and lower than those of the dry surface respectively. Moreover, equations are developed for predicting the *f* and the *j* factors of a tested heat exchanger. Results from the developed equations agree well with the experimental data.

Key words : air-side performance, dehumidification, crimped spiral fins

[1]Ph.D.(Thermal Technology), Engineer Level 6, Mae Moh Training Center, Electricity Generating Authority of Thailand, Mae Moh, Lampang 52220 [2]D.Eng.(Energy Technology), Prof., Department of Mechanical Engineering, Chiang Mai University, Chiang Mai 50202, Thailand.
Corresponding e-mail: atipoang.n@egat.co.th
Received, 8 January 2004 Accepted, 27 February 2004

บทคัดย่อ

อติพงศ์ นันทพันธุ์ [1] และ ทนงเกียรติ เกียรติศิริโรจน์ [2]

พฤติกรรมทางความร้อนของกลุ่มท่อติดครีบแบบเกลียวชนิดขอบหยักภายใต้สภาวะการควบแน่นของไอน้ำ: กรณีศึกษาการจัดเรียงท่อในแนวเดียวกัน

ว. สงขลานครินทร์ วทท. 2547 26(4) : 509-519

งานวิจัยนี้ได้ศึกษาสมรรถนะเครื่องแลกเปลี่ยนความร้อนแบบไหลตามขวางที่ใช้ครีบเกลียวชนิดขอบหยักและจัดเรียงกลุ่มท่อในแนวเดียวกันภายใต้สภาวะของการเกิดการควบแน่นของไอน้ำในอากาศบนพื้นผิวเครื่องแลกเปลี่ยนความร้อน โดยได้ศึกษาอิทธิพลของขนาดของท่อ ระยะห่างระหว่างครีบ ความสูงของครีบ และรูปแบบการจัดเรียงท่อที่มีต่อสมรรถนะของระบบ จากการทดลองพบว่าคุณลักษณะการถ่ายเทความร้อนและความดันอากาศตกคร่อมเครื่องแลกเปลี่ยนความร้อนภายใต้สภาวะที่มีการควบแน่นของไอน้ำในอากาศจะใกล้เคียงกับสภาวะที่ไม่มีการควบแน่นของไอน้ำ แต่อย่างไรก็ตามพบว่าค่าสัมประสิทธิ์การถ่ายเทความร้อนและค่าความดันอากาศตกคร่อมเครื่องแลกเปลี่ยนความร้อนของกรณีศึกษานี้ต่ำกว่าและสูงกว่ากรณีที่ไม่มีการควบแน่นของไอน้ำตามลำดับ นอกจากนี้ยังได้ทำการพัฒนาสมการสหสัมพันธ์เพื่อใช้คำนวณค่าความดันอากาศตกคร่อม และค่าสัมประสิทธิ์การถ่ายเทความร้อนเครื่องแลกเปลี่ยนความร้อน ซึ่งสมการที่พัฒนาขึ้นสามารถใช้ทำนายผลการทดลองได้เป็นอย่างดี

[1]กองศูนย์ฝึกอบรมแม่เมาะ การไฟฟ้าฝ่ายผลิตแห่งประเทศไทย อำเภอแม่เมาะ จังหวัดลำปาง 52220 [2]ภาควิชาวิศวกรรมเครื่องกล คณะวิศวกรรมศาสตร์ มหาวิทยาลัยเชียงใหม่ อำเภอเมือง จังหวัดเชียงใหม่ 50200

The cross flow heat exchanger plays an important role in waste heat recovery process, especially, in economizers where flue gas exchanges heat with water. Normally, water flows inside the tube while hot gas flows outside. Because the heat transfer resistance at gas-side dominates the heat transfer of heat exchanger, many attempts have been carried out to improve the gas-side heat transfer. Circular fins or spiral fins are normally used for recovering heat from flue gas. In this study, the crimped spiral fin was taken and the detail of crimped spiral finned tube is shown in Figure 1. It should be noticed that the inner crimped edge gives a good attachment between the fins and the tube.

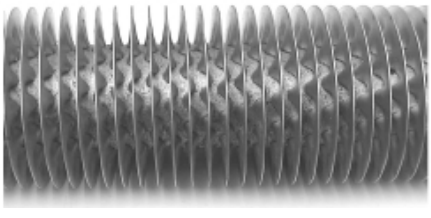

Figure 1. The crimped spiral fin.

When using a set of crimped spiral finned tubes in a cross flow heat exchanger, the designer should be concerned about the heat transfer coefficient and the gas or air stream pressure drop of the tube bank. Many research works have been performed to find out these values, such as Briggs and Young (1963), Robinson and Briggs (1966), Rabas *et al*. (1981) and Schmidt (1963) in the case of circular finned tube bank and Nuntaphan and Kiatsiriroat (2003) in the case of crimped spiral fins. However, these studies dealt with the dry coil conditions. Actually, in the case of waste heat recovery system, the heat exchanger is faced with condensation of moisture in the hot gas or air stream at the heat exchanger surface. Although the designer tries to avoid this condition because the finned tube might be corroded, in case of small boilers, condensation of moisture always occurs. There are very few reports about the performance of the tube bank particularly the cross flow heat exchanger using crimped spiral finned especially in case of inline arrangement. Despite of its comparatively low heat transfer performance, its lower pressure drop and high reliability (easy to main-

tain and clean) are very attractive in very severe environment. Therefore, the aim of this work was to study the heat transfer and friction characteristic of cross flow heat exchanger using crimped spiral fin in case of inline arrangement. This heat exchanger is faced with vapor condensation. Moreover, the heat transfer and friction correlations are also developed in this work.

Eeperimental Set-up

Figure 2 presents the schematic of the experimental set-up. The hot air stream flows through the tube bank and the water at room temperature circulates inside the tubes. In this experiment, the water flow rate is kept constant at 8 L/min. An accurate water flow meter is used for the measurement with a precision of ±0.1 L/min. The inlet temperature of water is approximately 30ºC. Both the inlet and outlet temperatures of water are measured by a set of calibrated K-type thermocouples and a temperature data logger records these signals.

A 1.5 kW centrifugal air blower with a frequency inverter and a controllable range of 0.1-0.5 kg/s keeps air flowing across the heat exchanger. A standard nozzle and an inclined manometer measure the mass flow rate of the air stream with ±0.5 Pa accuracy. The inlet temperature of the air stream is kept constant at 65ºC by a set of heaters and a temperature controller. The inlet and the outlet dry bulb and wet bulb temperatures of the air stream are also measured by a number of K-type thermocouples which are positioned at various locations along the flow cross-sections. Note that all of the thermocouples have been calibrated to ±0.1ºC accuracy. The inclined manometer also measures the pressure drop across the heat exchanger with ±0.5 Pa accuracy.

A total of 10 crimped spiral fin heat exchangers having various geometric parameters are tested in this study. Table 1 lists the details of the tested samples. Relevant definitions of the geometrical parameters and also shown in Figure 3. The effects of tube diameter, fin height, fin spacing, fin thickness, and tube arrangements on the airside performance are examined accordingly.

Data Reduction

The heat transfer rate of cross flow heat exchanger under dehumidifying condition can be calculated as follows:

$$Q_a = \dot{m}_a (i_{a,in} - i_{a,out}), \quad (1)$$

$$Q_w = \dot{m}_w C_{pw} (T_{w,out} - T_{w,in}). \quad (2)$$

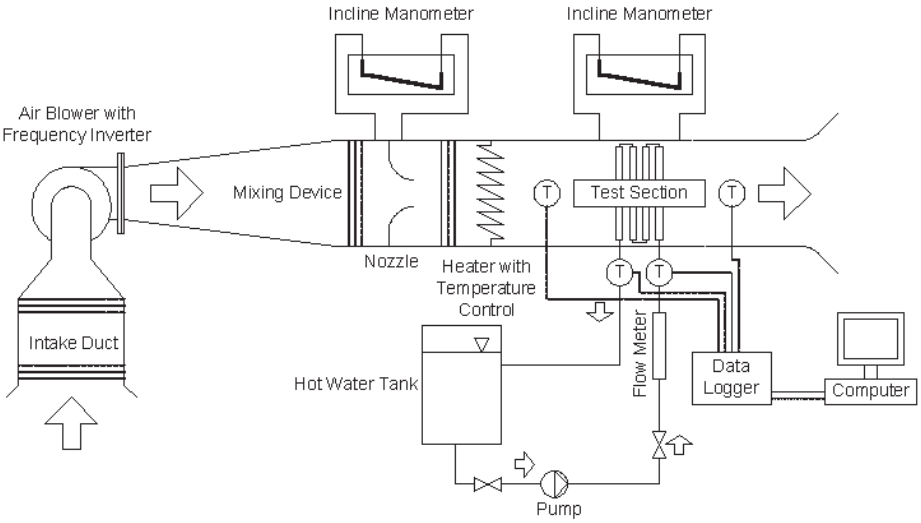

Figure 2. Schematic diagram of the experimental set-up.

Table 1. Geometric dimensions of cross flow heat exchanger

No	d_o (mm)	d_i (mm)	f_s (mm)	f_h (mm)	f_t (mm)	S_t (mm)	S_l (mm)	n_r	n_t	arrangement
1	17.3	13.3	3.85	10.0	0.4	50.0	50.0	4	10	inline
2	27.2	21.6	3.85	10.0	0.4	50.0	50.0	4	10	inline
3	21.7	16.5	6.10	10.0	0.4	50.0	50.0	4	10	inline
4	21.7	16.5	3.85	10.0	0.4	50.0	50.0	4	10	inline
5	21.7	16.5	2.85	10.0	0.4	50.0	50.0	4	10	inline
6	21.7	16.5	3.85	10.0	0.4	71.4	50.0	4	7	inline
7	21.7	16.5	3.85	15.0	0.4	71.4	50.0	4	7	inline

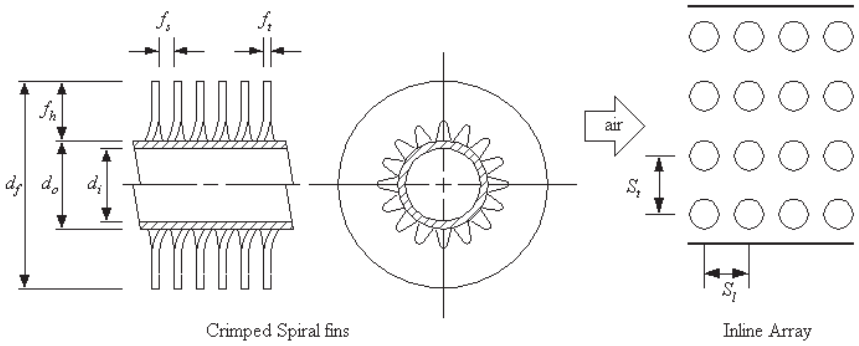

Figure 3. Relevant definitions of the geometrical parameters of crimped spiral fins.

Note that the heat transfer rates in Equation (1) and Equation (2) are the air-side and the tube-side, respectively. In this study, the average heat transfers rate can be evaluated as

$$Q_{avg} = 0.5(Q_a + Q_w). \tag{3}$$

The average heat transfer rate can be defined as a function of the overall heat transfer coefficient based on the mean enthalpy difference as

$$Q_{avg} = U_{o,w} A_o F \Delta i_m. \tag{4}$$

F is the correction factor in the case of cross flow unmixed/unmixed configuration.

Threlkeld (1970) defines the mean enthalpy difference for counter flow tube bank as

$$\Delta i_m = \frac{\left(i_{a,in} - i_{r,out}\right) - \left(i_{a,out} - i_{r,in}\right)}{\ln\left(\frac{i_{a,in} - i_{r,out}}{i_{a,out} - i_{r,in}}\right)}. \tag{5}$$

Mayer (1967) showed the relation of the overall heat transfer coefficient ($U_{o,w}$) and other heat transfer resistance as

$$\frac{1}{U_{o,w}} = \frac{b_r' A_o}{h_i A_{p,i}} + \frac{b_p' x_p A_o}{k_p A_{p,m}} + \frac{1}{h_{o,w}\left(\frac{A_{p,o}}{b_{w,p}' A_o} + \frac{A_f \eta_{f,wet}}{b_{w,m}' A_o}\right)}, \tag{6}$$

where

$$h_{o,w} = \frac{1}{\frac{C_{p,a}}{b_{w,m}' h_{c,o}} + \frac{y_w}{k_w}}. \tag{7}$$

Note that the ratio of water film thickness and thermal conductivity of water (y_w/k_w) is very small compared to other terms (1997) and they are neglected in this study.

The tube side heat transfer coefficient can be calculated from Gnielinski correlation (1976) as

$$h_i = \frac{(f_i/2)(\mathrm{Re}_{Di}-1000)\,\mathrm{Pr}}{1.07+12.7\sqrt{f_i/2}\left(\mathrm{Pr}^{2/3}-1\right)}\left(\frac{k_i}{d_i}\right), \quad (8)$$

where

$$f_i = \frac{1}{(1.58\ln \mathrm{Re}_{Di}-3.28)^2}. \quad (9)$$

The four quantities in Equation 7 can be estimated following the method of Wang *et al*. (1997) based on the enthalpy-temperature ratios. In case of $b_r^{'}$ and $b_p^{'}$, they can be calculated as

$$b_r^{'} = \frac{i_{s,p,i,m} - i_{r,m}}{T_{p,i,m} - T_{r,m}}, \quad (10)$$

$$b_p^{'} = \frac{i_{s,p,o,m} - i_{s,p,i,m}}{T_{p,o,m} - T_{p,i,m}}. \quad (11)$$

The quantity $b_{w,p}^{'}$ is the slope of saturated enthalpy curve evaluated at the outer mean water film temperature at the base surface and in case of no loss, it can be approximated from the slope of the saturated enthalpy curve evaluated at the base surface temperature of the tube. However, the quantity $b_{w,m}^{'}$, which is defined as the slope of the saturated enthalpy curve evaluated at the outer mean water film temperature at the fin surface, cannot be calculated directly. Consequently, the trial and error procedure is selected to find out this value. Wang *et al*. (1997) also gave the steps of this method as follows:

1. Assume a value of $T_{w,m}$ and calculate the quantity $b_{w,m}^{'}$
2. Calculate $h_{o,w}$ from Equation 6
3. Calculate the quantity $i_{s,w,m}$ by this following relation

$$i_{s,w,m} = i - \frac{C_{p,a}}{b_{w,m}^{'}}\frac{h_{o,w}}{h_{c,o}}\eta_{f,wet}\times\left(1-U_{o,w}A_o\left[\frac{b_r^{'}}{h_i A_{p,i}}+\frac{x_p b_p^{'}}{k_p A_{p,m}}\right]\right)\left(i-i_{r,m}\right). \quad (12)$$

4. Determine the new $T_{w,m}$ at $i_{s,w,m}$ and repeat the procedure again until the error is in limit.

The wet fin efficiency can be evaluated by the method of Wang *et al*. (1997) as:

$$\eta_{f,wet} = \frac{2r_i}{M_T\left(r_o^2-r_i^2\right)}\times\left[\frac{K_1(M_T r_i)I_1(M_T r_o)-K_1(M_T r_o)I_1(M_T r_i)}{K_1(M_T r_o)I_o(M_T r_i)+K_o(M_T r_i)I_1(M_T r_o)}\right], \quad (13)$$

where

$$M_T = \sqrt{\frac{2h_{o,w}}{k_f f_t}} = \sqrt{\frac{2h_{c,o}}{k_f f_t}}\sqrt{\frac{b_w^{'}}{C_{p,a}}}. \quad (14)$$

In this work, the sensible heat transfer coefficient ($h_{c,o}$) and pressure drop of air stream across tube bank are presented in term of the Colburn factor (j) and the friction factor (f) factors as

$$j = \frac{h_{c,o}}{G_{\max}C_{p,a}}\mathrm{Pr}^{2/3}, \quad (15)$$

$$f = \frac{A_{\min}}{A_o}\frac{\rho_i}{\rho_m}\left[\frac{2\rho_i\Delta P}{G_c^2}-\left(1+\sigma^2\right)\left(\frac{\rho_i}{\rho_o}-1\right)\right]. \quad (16)$$

Results and Discussion

Sensible Heat Transfer Coefficient

Figure 4 shows the effect of tube diameter on the sensible heat transfer coefficient at various

frontal velocities of air stream. The fin spacing (3.85 mm), fin thickness (0.4 mm), and the fin height (10 mm) are taken for this comparison. The transverse and the longitudinal tube pitches are 50 mm. As expected, the heat transfer coefficient rises with the frontal velocity. However, it is interesting to note that the heat transfer coefficient increases with the reduction of tube diameter. This phenomenon is attributed to the ineffective area behind the tube which increases with the tube diameter especially, the inline arrangement. Wang *et al*. (2002) performed flow visualizations via dye injection technique for fin-and-tube heat exchangers having inline arrangement. Their visual results unveil a very large flow circulation behind the tube row. Consequently this large recirculation contribute not only to the decrease of heat transfer coefficient but also to the rise of pressure drop. In addition, the large recirculation may also block the subsequent tube row and degrades the heat transfer performance hereafter.

Figure 5 shows the effect of fin height on the airside performance for inline arrangement. In this comparison, the associated fin heights are 10 and 15 mm and the fin spacing and the tube diameter are 3.85 mm and 21.7 mm and the transverse and the longitudinal pitches are 71.4 and 50 mm, respectively. As seen in the figure, the influence of fin height shows tremendous influence on the heat transfer performance. The heat transfer coefficients drop drastically with the increase of fin height. This is probably due to the airflow bypass effect. Actually the airflow is prone to flowing in the portion where the flow resistance is small. In case of f_h = 15 mm, the airflow resistance around fin tube is larger than that for f_h = 10 mm. Therefore, part of the directed airflow just bypasses the tube row without effective contribution to the heat transfer and lower heat transfer coefficient is obtained.

The effect of the fin spacing on the airside performance is shown in Figure 6. It was found that the increase of fin spacing gives a rise to the heat transfer coefficient. An explanation of this phenomenon is the same as that in the previous case which concludes that the result comes from the airflow bypass effect. The result of airflow bypass effect is also shown in Figure 7. It can be seen that the high transverse tube pitch (S_t = 71.4 mm) gives lower heat transfer coefficient than that of the low value (S_t = 50 mm).

Comparison of the heat transfer coefficient under dehumidifying process with that of non-dehumidifying condition from the report of Nuntaphan and Kiatsiriroat (2003) is also shown in Figures 4-7. The heat transfer phenomena of the wet surface heat exchanger are close to those of the dry surface. However, the heat transfer coefficient of the wet surface is lower than that of dry surface. Actually, there are many reports showing the comparison of the heat transfer coefficient between wet and dry surface heat exchanger. Some experiments show the heat transfer augmentation of wet surface, such as Meyers (1967), Elmahdy (1975) and Eckels and Rabas (1987) for the continuous plate finned tube. However, some reports show a decreased heat transfer coefficient of the wet surface, such as for the wavy finned tube. Mirth and Ramadhyani (1993) showed 17-50% decreasing of heat transfer coefficient of wet surface. Moreover, Wang *et al*. (1997) showed a decrease in the Colburn *j* factor of plate finned tube when the Reynolds number was lower than 2,000. However, at the higher Reynolds number, the *j* factor of wet surface is slightly higher than that of dry surface. The present results are generally in agreement with the trend of Wang *et al*. (1997).

In this research, the correlation for predicting the Colburn *j* factor including the effect of various quantities is also developed and the model is

$$j = 0.0023 Re_D^m \left(\frac{d_o}{S_t}\right)^{-5.8433} \left(\frac{f_t}{f_s}\right)^{-0.6457} \left(\frac{S_l}{S_t}\right)^{2.9009} \left(\frac{d_o}{d_f}\right)^{8.6111}, \quad (17)$$

where

$$m = 0.4987 + 1.0593\left(\frac{d_o}{S_t}\right) + 0.4265\left(\frac{f_t}{f_s}\right) - 1.8579\left(\frac{d_o}{d_f}\right). \quad (18)$$

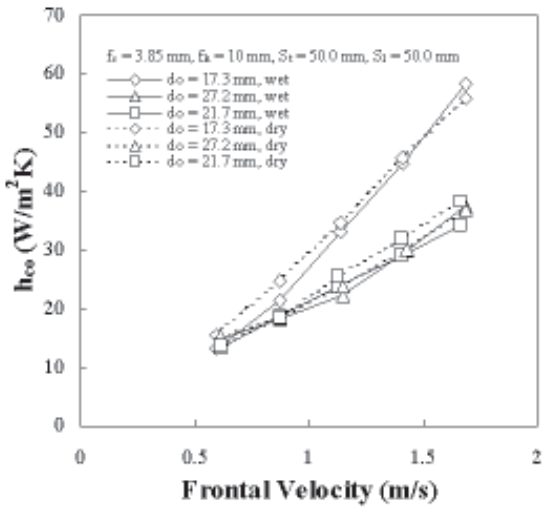

Figure 4. Effect of tube diameter on the sensible heat transfer coefficient.

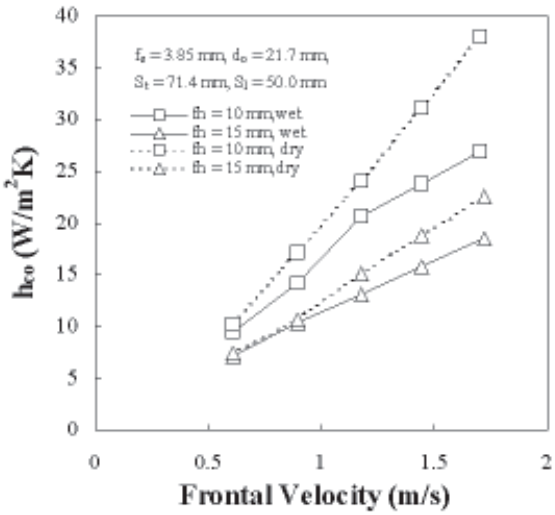

Figure 5. Effect of fin height on the sensible heat transfer coefficient.

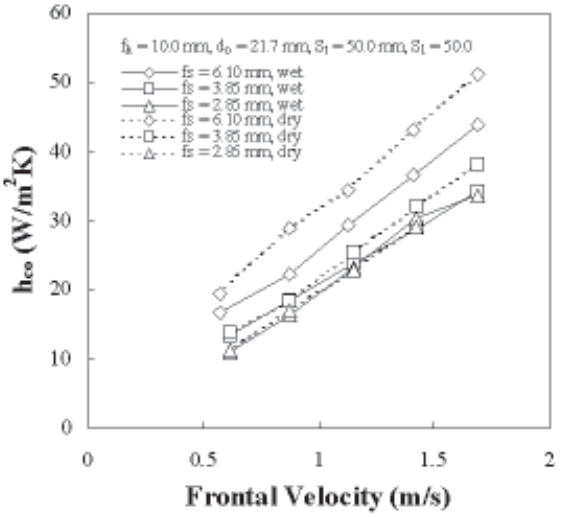

Figure 6. Effect of fin spacing on the sensible heat transfer coefficient.

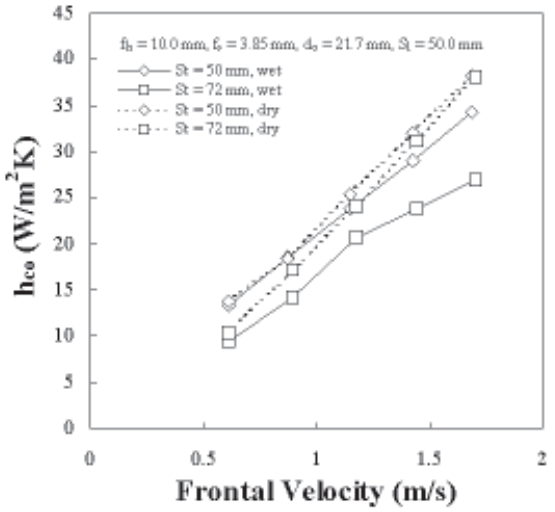

Figure 7. Effect of transverse pitch on the sensible heat transfer coefficient.

It is found that the *j* model can predict about 85.7% of the experimental data within ±15% accuracy. The comparison is also shown in Figure 8.

Pressure Drop

Figures 9-12 show the air stream pressure drops in the cross flow heat exchanger. It is found that the air stream pressure drop increases with the frontal velocity of air. Moreover, when compare with the result obtained from Nuntaphan and Kiatsiriroat (2003) in the case of dry surface heat exchanger, the pressure drop is slightly higher than that of dry surface. This is because only small amount of water vapor is condensed on the heat exchanger surface.

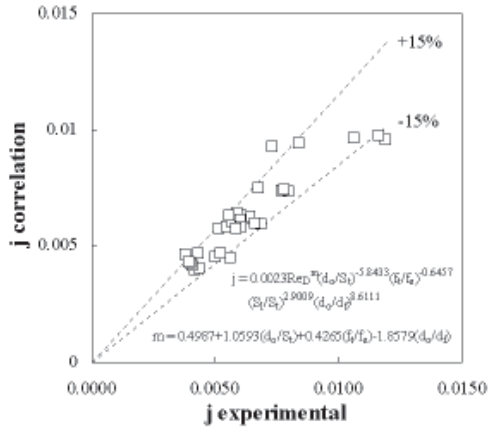

Figure 8. The comparison of *j* factor from experiment and correlation.

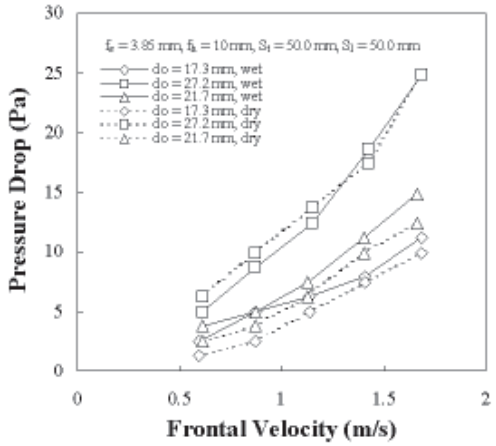

Figure 9. Effect of tube diameter on the pressure drop.

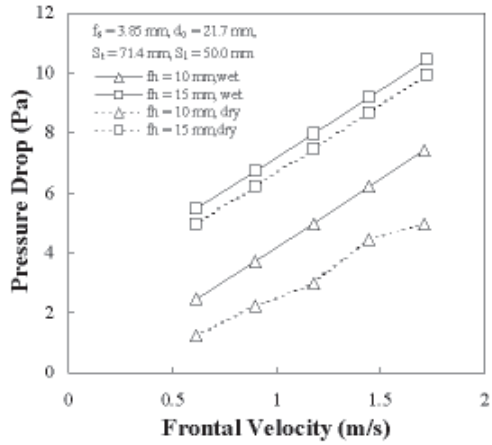

Figure 10. Effect of fin height on the pressure drop.

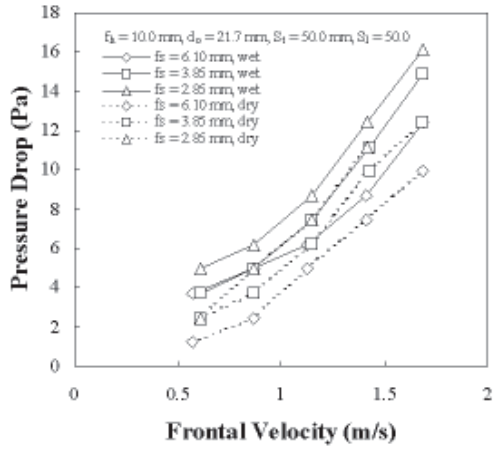

Figure 11. Effect of fin spacing on the pressure drop.

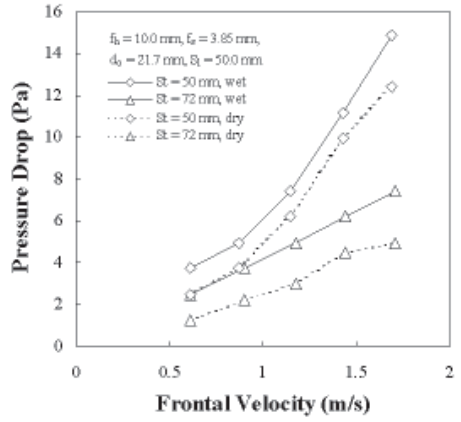

Figure 12. Effect of transverse pitch on the pressure drop.

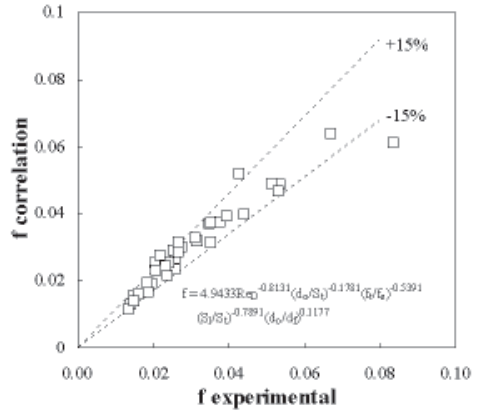

Figure 13. The comparison of f factor from experiment and correlation.

Figures 9-11 also show the pressure drop increases with tube diameter (d_o) and fin height (f_h). However, it decreases with increasing fin spacing (f_s). These phenomena come from the increasing of surface area resulting in higher air-flow resistance. The effect of tube arrangement is also seen in Figure 12. Higher transverse pitch of tube bank gives lower pressure drop.

In this research, the correlation for predicting the air stream pressure drop including the effect of various quantities is also developed and the model is in the form of

$$f = 4.9433 Re_D^{-0.8131} \left(\frac{d_o}{S_t}\right)^{-0.1781} \left(\frac{f_t}{f_s}\right)^{-0.5391} \left(\frac{S_t}{S_t}\right)^{-0.7891} \left(\frac{d_o}{d_f}\right)^{0.1177} . \quad (20)$$

From Figure 13, it is found that the *f* model can predict about 82.3% of the experimental data within ±15% accuracy.

Conclusion

From the experiment, it can be concluded as follows:

1. The heat transfer coefficient of wet surface is lower than that of dry surface.

2. The tube diameter, the fin height, the fin spacing and the transverse tube pitch of the cross flow heat exchanger under dehumidifying condition affect the heat transfer coefficient and the result is close to that of dry surface heat exchanger.

3. The air stream pressure drop of wet surface heat exchanger increases with the mass flow rate of air. The result is close to that of dry surface because only a small amount of vapor is condensed.

4. The developed models for predicting the *j* and the *f* factors can estimate about 85.7% and 82.3% of experimental data within ±15% accuracy.

Acknowledgement

The authors gratefully acknowledge the support provided by the Thailand Research Fund for carrying out this study.

References

Briggs, D.E. and Young, E.H. 1963. Convective Heat Transfer and Pressure Drop of Air Flowing Across Triangular Pitch Banks of Finned Tube, Chem. Engng. Prog. Sym. Series, 59(41): 1-10.

Eckels, P.W. and Rabas, T.J. 1987. Dehumidification: on the Correlation of Wet and Dry Transport Process in Plate Finned-tube Heat Exchangers, ASME J. of Heat Transfer, 109: 572-582.

Elmahdy, A.H. 1975. Analytical and Experimental Multi-row, Finned-tube Heat Exchagner Performance during Cooling and Dehumidification Process, Ph.D. thesis, Carleton University, Ottawa, Canada.

Gnielinski, V. 1976. New Equation for Heat and Mass Transfer in Turbulent Pipe and Channel Flow, Int. Chem. Engng, 16: 359-368.

McQuiston, F.C. 1978. Heat mass and Momentum Transfer Data for Five Plate-fin Tube Transfer Surface, ASHRAE Trans., Part 1, 84: 266-293.

McQuiston, F.C. 1978. Correlation of Heat mass and Momentum Transport Coefficients for Plate-fin Tube Transfer Surfaces with Staggered Tubes, ASHRAE Trans., Part 1, 84: 294-309.

Mirth, D.R. and Ramadhyani S. 1993. Prediction of Cooling-coils Performance Under Condensing Conditions, Int. J. of Heat and Fluid Flow, 14(4): 391-400.

Myers, R.J. 1967. The Effect of Dehumidification on the Air-side heat Transfer Coefficient for a Finned-tube Coil, M.S. Thesis, University of Minnesota, Minneapolis.

Nuntaphan, A. and Kiatsiriroat, T. 2003. Heat Transfer Characteristic of Cross Flow Heat Exchanger Using Crimped Spiral Fins a Case Study of Staggered arrangement, The 17th Conference of Mechanical Engineering Network of Thailand, Prachinburi, Thailand.

Rabas, T.J., Eckels, P.W. and Sabatino, R.A. 1981. The Effect of Fin Density on the Heat Transfer and Pressure Drop Performance of Low Finned Tube Banks, Chem. Engng. Coms., 10(2): 127-147.

Robinson, K.K. and Briggs, D.E. 1966. Pressure Drop of Air Flowing Across Triangular Pitch Banks of Finned Tubes, Chem. Engng. Prog. Sym. Series, 62(64): 177-184.

Schmidt, Th.E. 1963. Der Warmeubergeng an Rippenrohen und die Berechnung von Rohrundel Warme Austauschern, Kalttech, 15(4): 98; 15 (12): 370.

Threlkeld, J.L. 1970. Thermal Environmental Engineering, Prentice-Hall Inc., New York, USA.

Wang, C.C., Hsieh, Y.C. and Lin, Y.T. 1997. Performance of Plate Finned Tube Heat Exchanger Under Dehumidifying Conditions, ASME J. of Heat Transfer, 119: 109-119.

Wang, C.C., Lou, J., Lin, Y.T. and Wei, C.S. 2002. Flow Visualization of Annular and Delta Winlet Vortex Generators in Fin-and-tube Heat Exchanger Application, Int. J. of Heat and Mass Transfer, 45: 3803-3815.

Nomenclature

A_{min} minimum free flow area

A_o total surface area

$A_{p,i}$ inside surface area of tube

$A_{p,m}$ mean surface area of tube

$A_{p,o}$ outside surface area of tube

b'_p slope of straight line between the outside and inside tube wall temperature

b'_r slope of the air saturation curved at the mean coolant temperature

$b'_{w,m}$ slope of the air saturation curved at the mean water film temperature of the external surface

$b'_{w,p}$ slope of the air saturation curve at the mean water film temperature of the primary surface

$C_{p,a}$ moist air specific heat at constant pressure

$C_{p,w}$ water specific heat at coolant pressure

d_f outside diameter of finned tube

d_i tube inside diameter

d_o tube outside diameter

f friction factor

f_h fin height

f_i in-tube friction factor of water

f_s fin spacing

f_t fin thickness

F correction factor

G_{max} maximum mass velocity based on minimum flow area

$h_{c,o}$ sensible heat transfer coefficient for wet coil

h_i inside heat transfer coefficient

$h_{o,w}$ total heat transfer coefficient for wet external fin

I_0 modified Bessel function solution of the first kind, order 0

I_1 modified Bessel function solution of the first kind, order 1

i air enthalpy

$i_{a,in}$ inlet air enthalpy

$i_{a,out}$ outlet air enthalpy

$i_{r,m}$ saturated air enthalpy at the mean refrigerant temperature

$i_{r,in}$ saturated air enthalpy at the inlet of refrigerant temperature

$i_{r,out}$ saturated air enthalpy at the outlet of refrigerant temperature

$i_{s,p,i,m}$ saturated air enthalpy at the mean inside tube wall temperature

$i_{s,p,o,m}$ saturated air enthalpy at the mean outside tube wall temperature

$i_{s,w,m}$ saturated air enthalpy at the mean water film temperature of the external surface

Δi_m mean enthalpy difference

j the Colburn factor

K_0 modified Bessel function solution of the second kind, order 0
K_1 modified Bessel function solution of the second kind, order 1
K_f thermal conductivity of fin
K_i thermal conductivity of tube side fluid
K_p thermal conductivity of tube
K_w thermal conductivity of water
m parameter
$\dot{m}_a$ air mass flow rate
$\dot{m}_w$ water mass flow rate
n_r number of tube row
n_t number of tube in each row
ΔP pressure drop
Pr Prandtl number
Q_{avg} mathematical average heat transfer rate
Q_a air-side heat transfer rate
Q_w water side heat transfer rate
r_i distance from the center of the tube to the fin base
r_o distance from the center of the tube to the fin tip
Re_{Di} Reynolds number based on inside diameter of bare tube
Re_D Reynolds number based on outside diameter of bare tube
S_l longitudinal tube pitch
S_t transverse tube pitch
$T_{w,m}$ mean temperature of water film
$T_{w,in}$ water temperature of at the tube inlet
$T_{w,out}$ water temperature of at the tube outlet
$T_{p,i,m}$ mean temperature of the inner tube wall
$T_{p,o,m}$ mean temperature of the outer tube wall
$T_{r,m}$ mean temperature of refrigerant coolant
$U_{o,w}$ overall heat transfer coefficient
x_p thickness of tube wall
y_w thickness of condensate water film
$\eta_{f,wet}$ wet fin efficiency
ρ_i mass density of inlet air
ρ_o mass density of outlet air
ρ_m mean mass density of air
σ contraction ratio